

# Design of Dual-Emitting Nonaromatic Fluorescent Polymers through Thermal Processing of L-Glutamic Acid and L-Lysine

Marta Cadeddu, Davide Carboni,\* Luigi Stagi, Luca Malfatti, Maria F. Casula, Francesca Caboi, and Plinio Innocenzi\*



Cite This: *Macromolecules* 2024, 57, 514–527



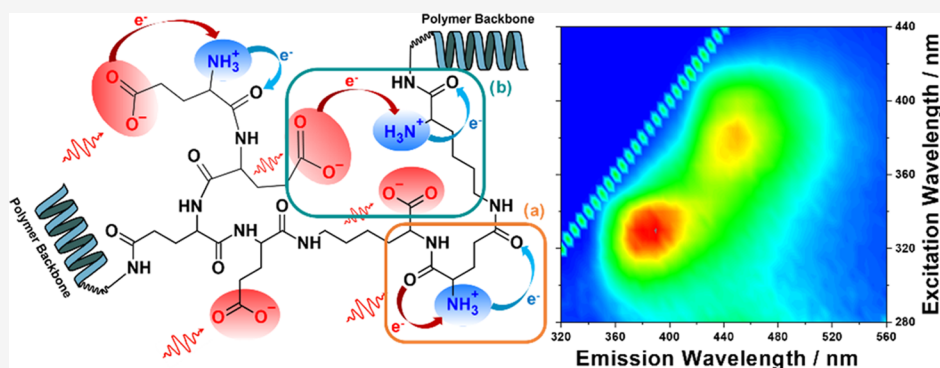
Read Online

ACCESS |

Metrics & More

Article Recommendations

Supporting Information



**ABSTRACT:** Fluorescence emission of proteins containing aromatic groups and conjugated bonds is generally associated with light absorption in the ultraviolet range, around 185–320 nm. Photoluminescence in nonaromatic biopolymers, however, has also been observed in amyloid-like structures and polymers derived from L-lysine and glycine. Here, we show, for the first time, that branched polymers obtained through thermal copolymerization of two nonaromatic amino acids, L-lysine and L-glutamic acid, exhibit two-color centers with relative absorptions in the visible range. Thermal homopolymerization of L-lysine or L-glutamic acid gives rise to the formation of branched polyglutamic acid and polylysine with a single fluorescence emission peaking at around 450 nm. The coreaction of the two amino acids produces instead a branched peptide-like polymer with a new emission centered at around 380 nm. The structures of the copolymers were studied by differential scanning calorimetry, in situ temperature-resolved FTIR, NMR, and TEM spectroscopy techniques. The optical properties were investigated by UV–vis and fluorescence spectroscopy. The double emission can be correlated with two different intramolecular charge transfer processes between the polymer backbone and the oppositely charged moieties of the two precursor side chains, Lys and Glu, which are at the origin of near-UV fluorescence.

## INTRODUCTION

The formation of fluorescent polymers from nonaromatic amino acids is a fascinating area of research that provides new insights into the chemical physical phenomena of luminescent nanomaterials.<sup>1–3</sup> UV–vis (185–320 nm) absorption in proteins is a well-known phenomenon that is generally attributed to the presence of aromatic amino acids, disulfide bonds, or polyconjugate carbon bonds.<sup>4</sup> More recently, evidence has emerged that organic polymers synthesized from nonaromatic amino acids, such as L-lysine, can also emit in the visible range.<sup>5,6</sup> Absorption and fluorescence beyond 250 nm in proteins, polypeptides, and branched polymers derived from amino acids lacking polyconjugate or aromatic bonds have now good experimental evidence, even if a clear understanding of the luminescence origin is still lacking.<sup>7,8</sup>

Our research group has experimentally demonstrated that polymers with strong emission in the blue region can be obtained from nonaromatic amino acids such as L-lysine<sup>2</sup> and

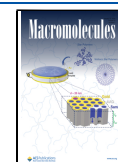
glycine.<sup>9</sup> L-lysine, in particular, forms branched and hyperbranched structures via thermal polymerization. These polymers are chromophores and exhibit well-defined lifetime, quantum yield, and correlated absorption–emission spectra. This fluorescence emission is strictly correlated to the formation of branched and hyperbranched polymers from the amino acid. A closely packed structure in hyperbranched polymers gives a more rigid conformation, while the constraints of the chains favor the interactions between nearby species through hydrogen bonding, promoting intramolecular charge transfer. The process can be used to obtain polymers

**Received:** September 8, 2023

**Revised:** December 11, 2023

**Accepted:** December 18, 2023

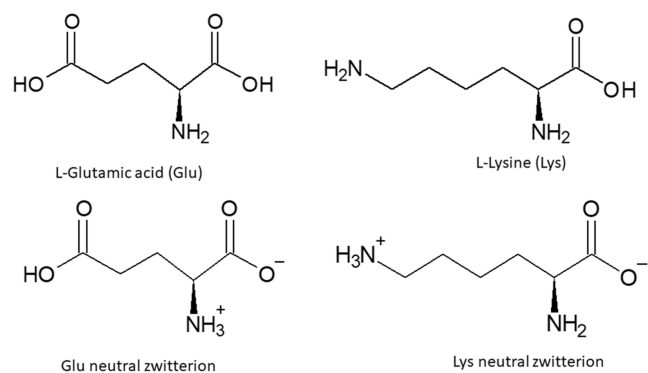
**Published:** January 5, 2024



with a high degree of branching that are also efficient emitters. However, the possibility of synthesizing fluorescent polymers from amino acids is still largely unexplored. An interesting question is what the optical properties of polymers would be if obtained by coreacting different types of amino acids. To answer this question, we have synthesized branched polymers by thermally coreacting two bifunctional amino acids, L-lysine and L-glutamic acid, in different molar ratios with the purpose of investigating whether any peculiar emission could be derived by their mutual interactions.

L-Glutamic acid (Glu) is a nonessential amino acid characterized by two carboxyl groups ( $\alpha$  and  $\delta$ ) and one amine group (Figure S1). In the solid state, the molecule assumes the neutral zwitterionic structure,<sup>10</sup> with the amine group protonated and the  $\alpha$ -carboxyl group deprotonated (Scheme 1).

**Scheme 1. Neutral and Zwitterionic Structures of L-Glutamic Acid and L-Lysine**



L-Lysine (Lys) is a physiologically charged amino acid bearing a carboxyl group, an  $\alpha$ -amino group, and an aliphatic side chain with a terminal amine ( $\epsilon$ -amine) (Figure S1). In the liquid state, Lys can be found in the anionic, cationic, or zwitterionic form as a function of pH. At physiological conditions, Lys assumes a zwitterionic form with protonated amino and deprotonated carboxyl groups. In the solid state, Lys is a neutral zwitterion<sup>11</sup> (Scheme 1).

Thermal polymerization of a properly catalyzed simple amino acid, such as L-lysine, has proven to be very effective in producing fluorescent bioactive nanostructured polymers with antiviral properties.<sup>6</sup> L-Lysine follows specific polymerization pathways due to the presence of the  $\alpha$  and  $\epsilon$  amino groups capable of forming branched and hyperbranched polymers through thermal amidation with and without boric acid as the catalyst.<sup>6</sup> On this basis, two different questions were addressed: first, the possibility of pursuing an approach similar to Lys but starting with an amino acid, L-glutamic acid, which is characterized by a chemical feature opposite to Lys, owing to the presence of an extra carboxylic group in addition to the fundamental amino acid moiety, and second, the investigation of the characteristics of new nanostructured materials obtained by thermally coreacting nonaromatic amino acids. The results show that the GluLys heteropolymers exhibit very peculiar properties not detected in the Lys and Glu homopolymers.

## EXPERIMENTAL SECTION

**Chemicals.** L-Glutamic acid ((S)-aminopentanedioic acid) powder ( $\geq 99\%$ ,  $\text{HO}_2\text{CCH}_2\text{CH}_2\text{CH}(\text{NH}_2)\text{CO}_2\text{H}$ ) and L-lysine ((S)-2,6-diaminocaproic acid) powder (crystallized,  $\geq 98.0\%$  (NT),  $\text{H}_2\text{N}-$

$(\text{CH}_2)_4\text{CH}(\text{NH}_2)\text{CO}_2\text{H}$ ) were purchased from Sigma-Aldrich, St. Louis (MO). All chemicals were used without further purification. Milli-Q water was used for the synthesis and analysis. The purification was carried out using benzoated membranes from dialysis tubing (average flat width 32 mm, 1.27 inch, molecular weight cutoff = 2000 Da, Sigma-Aldrich, St. Louis, MO).

**Material Synthesis. Poly-L-Glu (PGA) Homopolymer.** L-Glutamic acid (2g, 13.59 mmol) was placed in an oven using a ceramic crucible as the container, heated at a heating rate of  $10\text{ }^\circ\text{C min}^{-1}$  up to  $240\text{ }^\circ\text{C}$ , left at the target temperature for 5 h, and allowed to cool down to  $20\text{ }^\circ\text{C}$  before any further treatment. The obtained brown-black solid was dispersed in Milli-Q water, sonicated for 30 min, and then centrifuged at 9000 rpm for 20 min. The supernatant was collected, filtered using a  $0.45\text{ }\mu\text{m}$  syringe filter (Whatman Puradisc 30/0.45), and dialyzed against Milli-Q water for 24 h using a dialysis tube, replacing the water every 12 h. The resulting solution was then freeze-dried for 24 h and lyophilized with a Lio SP device.

**Poly-Lysine (Poly-Lys).** L-Lysine (2g, 13.68 mmol) was synthesized following the same procedure as that used for PGA.

**Poly-L-Glu-Lys Heteropolymers (Glu-Lys).** L-Glutamic acid and L-lysine powders were mixed in a mortar in different molar ratios: 1:1 (1.006 g + 1.000 g, 6.84 mmol + 6.84 mmol), 2:1 (2.012 g + 1.000 g, 13.68 mmol + 6.84 mmol), 3:1 (3.018 g + 1.000 g, 20.52 mmol + 6.84 mmol), and 1:3 (1.006 g + 3.000 g, 6.84 mmol + 20.52 mmol). The resulting mixture was then placed in a ceramic crucible and treated following the same procedure as described for the synthesis of PGA and Poly-Lys (vide supra). The yields of the thermal polymerization are reported in Table S1 of the Supporting Information.

**Material Characterization.** A combined thermogravimetric analysis–differential scanning calorimetry (TGA–DSC) analysis was performed using an SDT Q600 (TA Instruments). All analyses were performed under a  $\text{N}_2$  inert atmosphere (flow rate  $20\text{ mL min}^{-1}$ ) at temperatures up to  $400\text{ }^\circ\text{C}$  and a  $10\text{ }^\circ\text{C min}^{-1}$  heating rate.

UV–vis absorption spectra were recorded using a Nicolet Evolution 300 UV–Vis spectrophotometer (Thermo Fisher) with a bandwidth of 1.5 nm.

Fourier transform infrared (FTIR) spectroscopy analysis was carried out using an infrared Vertex 70 interferometer (Bruker). The FTIR absorption spectra were recorded in the  $4000\text{--}400\text{ cm}^{-1}$  range with a  $4\text{ cm}^{-1}$  resolution and 32 scans. The spectra were acquired using a potassium bromide pellet (KBr,  $\geq 99.5\%$ , Fluka). In situ FTIR spectra of sample powders dispersed in a potassium bromide pellet (KBr, IR 99%, Sigma) were collected using an electrical heating jacket in the transmission geometry (Specac). The spectra were collected at temperatures from  $25\text{ }^\circ\text{C}$  with  $10\text{ }^\circ\text{C}$  heating steps up to  $240\text{ }^\circ\text{C}$ . Data analysis was performed using Origin software. Occasionally, spectra were corrected using Opus 6.5 and a rubberband function for the baseline (2 iterations maximum) and 7 smoothing points.

Fluorescence spectroscopy measurements were performed on a Horiba Jobin Yvon Fluoromax-3. 3D Photoluminescence (PL) maps of aqueous solutions were recorded from 250 to 700 nm. The same spectrofluorometer and identical parameter settings were used in all of the analyses. Photoluminescence quantum yield (QY) measurements were performed using the quanta  $\phi$  (HORIBA) integrating sphere accessory, attached to a “NanoLog” Horiba Jobin Yvon spectrofluorometer.

The photoluminescence quantum yield (QY%) was measured using the quanta- $\phi$  (HORIBA) integrating sphere attached to the “NanoLog” Horiba Jobin Yvon spectrofluorometer. Measurements were performed on aqueous solutions of the samples in the same fused silica cuvette. Samples were excited with a wavelength corresponding to their maximum excitation peak, and emissions were typically recorded from 300 to 600 nm.

All NMR spectra were recorded on a Bruker Advance III instrument at 400 MHz proton frequency using a Bruker multinuclear BBFO plus 5 mm probe. NMR 1D  $^1\text{H}$  and  $^{13}\text{C}$  and 2D  $^1\text{H}\text{--}^{13}\text{C}$  HSQC spectra were recorded at  $T = 298\text{ K}$  (Bruker BVT3200 temperature control unit) using JCH = 145 Hz. Deuterium oxide ( $\text{D}_2\text{O}$  99.9 atom % D + tetramethylsilane (TMS, 0.05% v/v)),

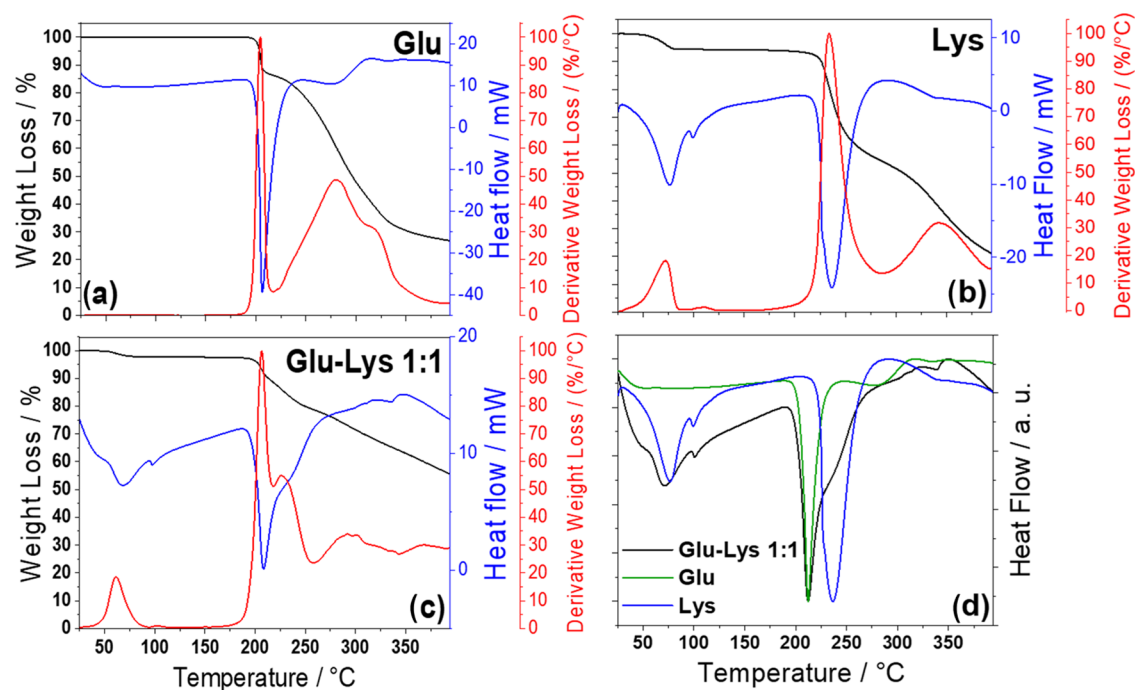
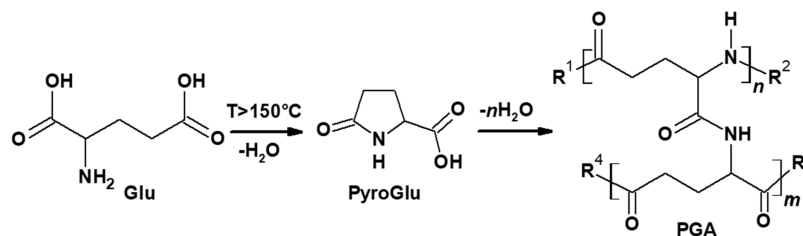


**Figure 1.** TGA–DSC profiles of L-glutamic acid (a), L-lysine (b), and Glu–Lys 1:1 (c) and the combined DSC normalized curves (d). The red curves are the first derivatives of the weight loss.

**Scheme 2. Dehydrocondensation Reaction of L-Glutamic Acid (Glu) to Form Pyroglutamic Acid (PyroGlu) and Subsequent Branched Polymerization That Gives Polyglutamic Acid (PGA)**



purchased from Sigma-Aldrich, was used as the solvent. Samples were dissolved in 0.6 mL of  $\text{D}_2\text{O}$  and transferred to a 5 mL NMR sample tube. TMS, used as the internal standard, was calibrated as  $\delta = 0.00$  ppm.

Transmission electron microscopy (TEM) investigation was performed by a JEM 1400 Plus TEM (Jeol Ltd., Japan) operating at 80 kV. Prior to observations, the sample dispersions were sonicated, dropped on a carbon-coated 200 mesh copper grid, and dried at  $50^\circ\text{C}$ .

X-ray diffraction (XRD) patterns of thin films were collected in grazing-incidence geometry using a Bruker D8 Discover diffractometer under irradiation with a  $\text{Cu K}\alpha_1$  line ( $=1.54056 \text{ \AA}$ ); the X-ray generator worked at a power of 40 kV and 40 mA. The patterns were recorded in  $2\theta$  ranging from  $10$  to  $70^\circ$  with a step size of  $0.02 \text{ \AA}$ .

## RESULTS

The present work has been triggered by the idea of investigating the optical properties of copolymers obtained through the thermal treatment of two nonaromatic amino acids without specific catalysts, with the specific purpose of getting a better understanding of the interplay between the functional groups characterizing the polymer side chains and its influence on the optical response. With this aim, L-glutamic acid was selected as a natural counterpart of L-lysine, given the opposite character of its side chain compared to L-lysine. Previous work in our laboratory has shown that thermal polymerization of L-

lysine, a fluorescent nonaromatic amino acid, characterized by the presence of a charged amino-propyl side chain, produces a hyperbranched polymer characterized by a single fluorescent blue emission.<sup>2</sup> Different from L-Lys, the L-Glu monomer shows a very weak fluorescent emission in the solid state but none in solution.

Since heat treatment plays a critical role in determining the thermal growth of the polymers and thus the final structure of the material, TGA–DSC analysis and in situ temperature-dependent FTIR spectroscopy have been used to optimize the synthesis process. The TGA–DSC analysis performed under a nitrogen atmosphere points out the changes occurring in the amino acid structures during the thermal treatment. The two amino acids independently, Lys and Glu, and an equimolar combination of the two, Glu–Lys 1:1, were studied (Figure 1).

Figure 1a shows the TGA–DSC profile of Glu as a function of the temperature up to  $400^\circ\text{C}$ . The curves have a good correspondence to those reported in a previous work.<sup>12</sup> Between  $200$  and  $220^\circ\text{C}$ , Glu shows an initial weight decrease of about  $12\%$ , corresponding to the loss of one water molecule per Glu unit and close to the theoretical value of  $12.24\%$ . After a small plateau, most of the weight loss,  $\sim 52\%$ , occurs from  $220$  to  $320^\circ\text{C}$ , and it is due to the intermolecular amidation and consequent formation of polyglutamic acid (PGA). The

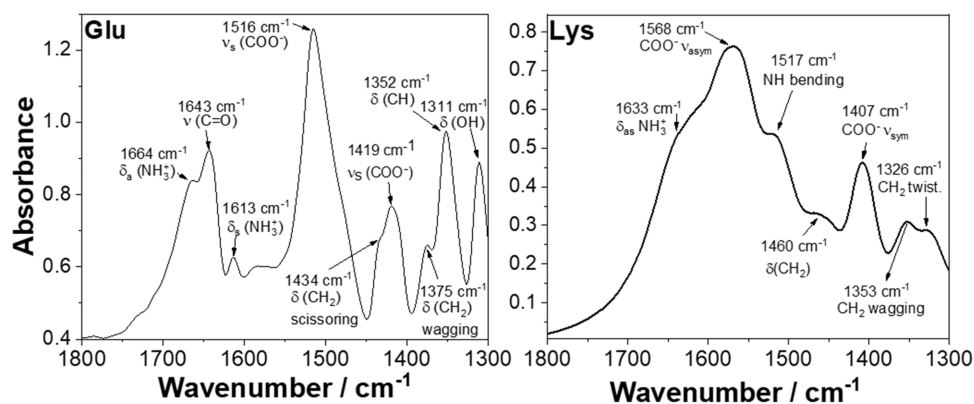


**Figure 2.** FTIR absorption spectra in the 1800–1300  $\text{cm}^{-1}$  interval of L-glutamic acid (Glu) and L-lysine (Lys) in the crystalline state.

sharp endothermic event peaking at 206  $^{\circ}\text{C}$  results from a combination of melting and dehydration–transformation reactions.<sup>13,14</sup> Two possible reactions have been associated with the thermal event at 206  $^{\circ}\text{C}$  and the loss of one molecule of  $\text{H}_2\text{O}$  per Glu unit: intramolecular dehydrocyclization that leads to the formation of pyroglutamic acid (PyroGlu) and a polymerization reaction to give polyglutamic acid (PGA) (Scheme 2).

The reaction that occurs between the amino group and the carboxylic moiety on the side chain forms an internal amide (a lactam), pyroglutamic acid, which is an intermediate step toward the formation of polyglutamic acid (PGA) whose rate of formation strictly depends on the heating conditions (temperature and time).<sup>14,15</sup>

The experiments have shown that the transformation from Glu to PGA occurs in 24 h at 150  $^{\circ}\text{C}$ . However, increasing the temperature to 170 $^{\circ}$  reduces the transformation time to 3 h.<sup>13</sup> In our experimental conditions, the transformation to PGA goes to completion by heating Glu for 5 h in air at 240  $^{\circ}\text{C}$ . It should be underlined, however, that pyroglutamic acid may act both as an activating species (initiator) that promotes polymerization and as a proper monomer that is involved in chain growth. Thanks to this dual function, PyroGlu can play this double role also during copolymerization with other amino acids,<sup>14,16,17</sup> and it can take the designation of “inomer” (initiator + monomer).

Between 220 and 350  $^{\circ}\text{C}$ , the TGA profile indicates the loss of about half of the total weight, while the DSC curve shows two small endothermic events peaking at 280 and 330  $^{\circ}\text{C}$ . These events are evidenced by the first derivative of the weight loss curve, which shows two peaks in correspondence with these same events. These findings can be correlated with the formation of polyglutamic acid (PGA) through a polycondensation reaction that starts predominantly at temperatures higher than 220  $^{\circ}\text{C}$ . In general, thermal-induced transformations of Glu in the 140–220  $^{\circ}\text{C}$  range are the result of a complex interplay of melting, dehydration, and structural reorganizations.

Figure 1b shows the TGA–DSC profiles of Lys. The first significant endothermic event peaks at 76  $^{\circ}\text{C}$  and is followed by a second one, which has a smaller intensity, peaking at 100  $^{\circ}\text{C}$ . Both events can be correlated to the loss of adsorbed water (about 5% weight loss corresponding to 0.5 mol water) during dehydration.<sup>18,19</sup> The main endothermic event peaks at 236  $^{\circ}\text{C}$  and overlaps with another endothermic process at 228  $^{\circ}\text{C}$ , which is detected as a shoulder. The combined events account for a weight loss of about 34%. The first thermal event at 228

$^{\circ}\text{C}$  is due to the melting of Lys, whose melting temperature is, in fact, 224.5  $^{\circ}\text{C}$ . The second one at 236  $^{\circ}\text{C}$  is associated with the intermolecular amidation between amino acid moieties, which is responsible for the formation of polymers with different degrees of branching.<sup>12</sup> At temperatures higher than 300  $^{\circ}\text{C}$ , carbonization takes place. Figure 1c shows the TGA–DSC profiles of Glu–Lys in a 1:1 ratio mixture. The TGA–DSC curves show that the thermal reactions of Glu and Lys follow the following sequence: melting of Glu, formation of pyroglutamic acid (intramolecular amidation), melting of Lys, and polymerization of Glu and Lys (intermolecular amidation) (Figure 1d).

To further clarify the structural transformations induced by the thermal treatments, we have performed FTIR and NMR analyses.

Figure 2a shows the FTIR absorption spectrum in the 1800–1300  $\text{cm}^{-1}$  range of Glu and Lys powders in the crystalline state. They have been used as a reference to monitor the change in the amino acid structure during the thermal treatment. This infrared region has a specific importance because it falls within the amide I and II regions and allows identifying the structure of the molecule. The full spectra are shown in Figure S1, and the attribution of the vibrational modes is listed in Tables S1 and S2.<sup>20–23</sup>

The FTIR spectrum shows that Glu in the solid state is present as neutral zwitterionic molecules, which crystallize in orthorhombic structures. The hydrogen bonds between the carboxylate and carboxylic groups ( $\text{O}-\text{H}\cdots\text{O}$ ) and between the ammonium group and an oxygen atom in the carboxylic or carboxylate group stabilize the crystalline structure. The detection of in-plane bending modes of protonated amines,  $\text{NH}_3^+$ , at 1664  $\text{cm}^{-1}$ ,  $\delta_{\text{as}}$ , and 1613  $\text{cm}^{-1}$ ,  $\delta_{\text{s}}$ , and the stretching modes of the deprotonated carboxylic groups,  $-\text{COO}^-$ , at 1516  $\text{cm}^{-1}$ ,  $\nu_{\text{s}}$  symmetric, and 1419  $\text{cm}^{-1}$ ,  $\nu_{\text{as}}$  antisymmetric, well supports the attribution<sup>19</sup> (Figure 2). The FTIR absorption spectrum of Lys also indicates the formation of a crystalline structure by molecules in the zwitterionic state in the precursor powder such as Glu. The zwitterionic nature is supported by the detection of  $\text{NH}_3^+$ , at 1633  $\text{cm}^{-1}$  (shoulder),  $\delta_{\text{as}}$ , and the stretching modes of the deprotonated carboxylic groups,  $-\text{COO}^-$ , at 1568  $\text{cm}^{-1}$ ,  $\nu_{\text{as}}$ , and 1407  $\text{cm}^{-1}$ ,  $\nu_{\text{s}}$ .

The change in structure with temperature has been followed in situ through infrared spectroscopy by heating the precursor crystalline powders of the two amino acids, Glu and Lys. The reactivity of the two precursors, Glu and Lys, is directly dependent on the heating conditions (temperature and time), and thus, it is important to understand how the thermal

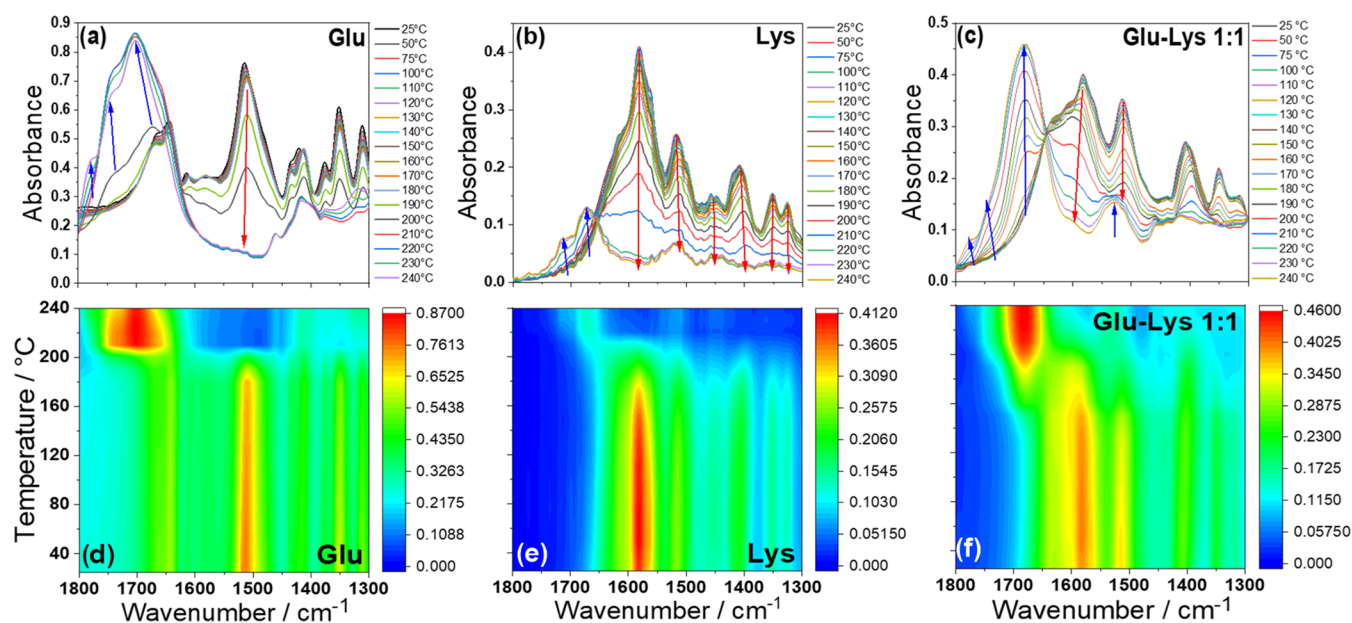


**Figure 3.** FTIR absorption spectra of Glu (a), Lys (b), and a mixture of Lys and Glu (Glu–Lys 1:1 molar ratio) (c) in the 1800–1300  $\text{cm}^{-1}$  range. The spectra have been recorded in situ as a function of the temperature from 25 up to 240  $^{\circ}\text{C}$  in air with a step size of 10  $^{\circ}\text{C}$  from 100  $^{\circ}\text{C}$ . Corresponding 3D maps ( $x$ , wavenumber;  $y$ , absorbance;  $z$ , false color scale intensity) for Glu (d), Lys (e), and Glu–Lys (f). The arrows are used to indicate the response of the band to the increase of temperature. The arrows pointing upward show the bands whose intensities increase with the temperature and vice versa.

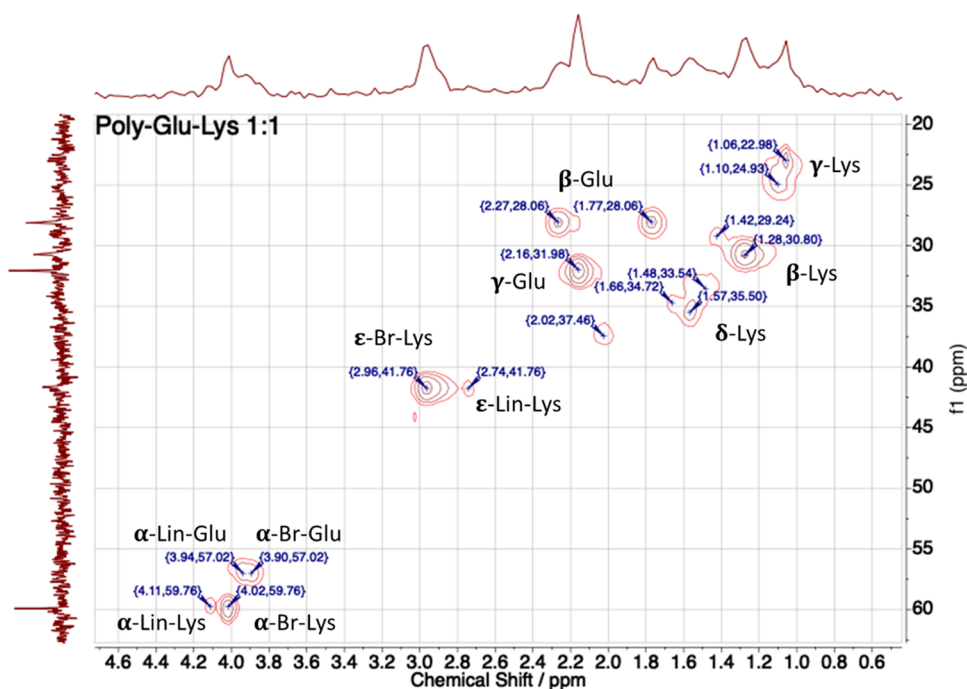


**Figure 4.**  $^1\text{H}$ – $^{13}\text{C}$  NMR HSQC spectrum of Glu–Lys 1:1 in  $\text{D}_2\text{O}$ . The Greek letters indicate the position of the hydrogens on the amino acid chain with respect to the main amino-carboxylic moiety ( $\alpha$ -CH). Prefixes **Br** and **Lin** indicate the branched and linear nature of the moieties, respectively.

treatment affects copolymerization. The in situ analysis gives direct information about the structural changes during thermal processing. For this purpose, the two amino acids alone, used as a reference, and the Glu–Lys 1:1 mixture have been analyzed as a function of temperature to identify when peculiar reactions may occur between the two monomers.

Figure 3 shows the FTIR absorption spectra of Glu (a), Lys (b), and a mixture of Lys and Glu (Glu–Lys 1:1 molar ratio)

(c) in the 1800–1300  $\text{cm}^{-1}$  range in 3D FTIR maps. The spectra have been recorded in situ as a function of the temperature from 25 up to 240  $^{\circ}\text{C}$  in air with a step size of 10  $^{\circ}\text{C}$  from 100  $^{\circ}\text{C}$ . The directions of the arrows are used to indicate the response of the bands to the increase of temperature (upward for the increase and downward for the decrease).

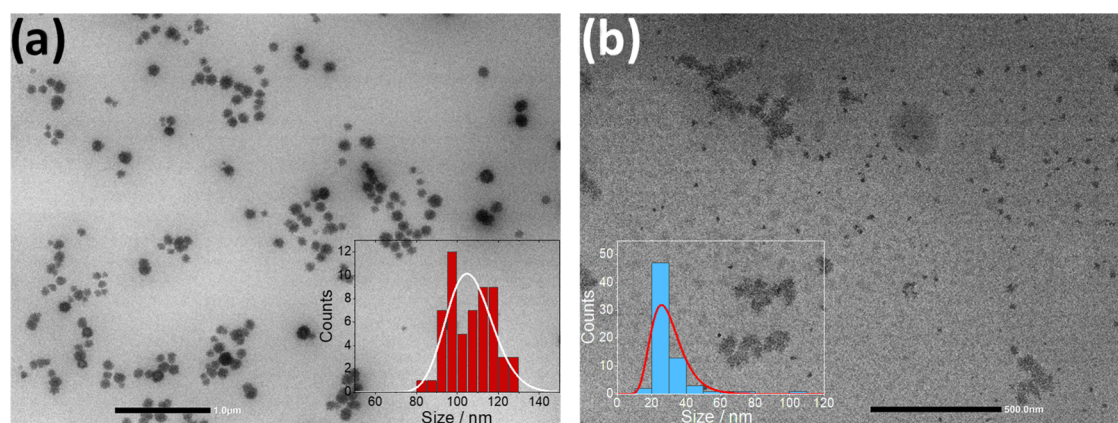


**Figure 5.** Bright-field Images of GluLys polymers at 1:1 (a) and GluLys 2:1 (b) ratios. The statistics on the size of the nanoparticles with the normal log trend are shown in the insets.

The sequential spectra as a function of temperature (Figure 3a–c), together with the 3D maps (Figure 3d–f), show the clear occurrence of an amidation reaction in all of the samples. The amidation reaction is marked in the 3D maps by the quick rise of the amide I and amide II bands at around 1700 and 1570  $\text{cm}^{-1}$ , respectively. The infrared spectra show that the amidation reaction occurs in a limited range of temperatures with a sudden change in the curve/color profiles. This temperature, however, varies in the three samples. In Glu, the intramolecular amidation starts at 190  $^{\circ}\text{C}$  and ends at 210  $^{\circ}\text{C}$ . This finding is in perfect agreement with what is observed in the TGA–DSC curves, which show that, in Glu, intra- and intermolecular amidations, ascribed to PyroGlu and PGA, respectively, span from 190 to 230  $^{\circ}\text{C}$ . In the case of Lys, however, amidation takes place at higher temperatures, starting at 210  $^{\circ}\text{C}$  and ending at about 260  $^{\circ}\text{C}$ , beyond the experimental capabilities of the apparatus that can perform analyses only up to 240  $^{\circ}\text{C}$ .

Copolymerization of Glu and Lys shows a pattern that appears like a combination of two single profiles with some distinctions. The monomer reaction starts with the intramolecular amidation of Glu into PyroGlu at temperatures as low as 150  $^{\circ}\text{C}$  and proceeds with the reaction between amines and carboxyl groups, which results in oligomer formation and polymerization (intermolecular amidation). The whole process moves gradually toward full polymerization, but it seems to end at lower temperatures. This could be, most probably, due to the Lys monomer that starts reacting at temperatures lower than its melting point because it is well dispersed into the as-formed viscous PyroGlu.

In Glu (Figure 3a), the carbonyl  $\text{C}=\text{O}$  stretching vibrations from carboxylate ( $1643\text{ cm}^{-1}$ ) to free acids or amide I ( $\text{COOH}$ ,  $1701\text{ cm}^{-1}$ ) and polyanhydride ( $1737\text{ cm}^{-1}$ ) are observed.<sup>24</sup> At temperatures higher than 220  $^{\circ}\text{C}$ , PGA begins to form.<sup>25</sup> The formation of the peptide bonds is more evident in Figure 3c, where the signal attributed to NH bending of the free amine ( $1514\text{ cm}^{-1}$ ) is displaced to form the amide II band ( $1529\text{ cm}^{-1}$ ). Moreover, the antisymmetric stretching of carboxylate ( $1581\text{ cm}^{-1}$ ) progressively decreases in intensity as the temperature increases due to the amidation reaction, while the signals at 1684, 1743, and  $1776\text{ cm}^{-1}$  increase from 150  $^{\circ}\text{C}$  onward. These bands are attributed to the free  $\text{C}=\text{O}$  stretching of amide I. The 3D map in Figure 3f illustrates this transformation effectively, which is evidenced by the red stripe in the false color scale centered at  $1581\text{ cm}^{-1}$  fading

progressively out in favor of another intense red stripe centered at  $1683\text{ cm}^{-1}$ .

After the thermal treatment, both PGA and Glu–Lys 1:1 polymers underwent several steps of purification, in particular dialysis against water, to remove some of the hydrolyzable byproducts together with occasional unreacted precursors, as evidenced from the change of the FTIR signal profiles of the samples (see Figure S2).

The nature of the polymers was also characterized by  $^1\text{H}$  NMR,  $^{13}\text{C}$  NMR, and  $^1\text{H}$ – $^{13}\text{C}$  NMR bidimensional heteronuclear correlation (HSQC) (Figure 4). The  $^1\text{H}$  NMR spectrum of the L-glutamic acid monomer in  $\text{D}_2\text{O}$  (Figure S3), taken as a reference, shows the  $\alpha$ -CH (t,  $^1\text{H}$ , 3.80 ppm,  $J_1 = 6.4\text{ Hz}$ ),  $\beta$ - $\text{CH}_2$  (td, 2H, 2.54 ppm,  $J_1 = J_2 =$ ), and  $\gamma$ - $\text{CH}_2$  (m, 2H, 2.14 ppm) chemical shifts. As a reference for L-lysine  $^1\text{H}$  NMR, we have used the spectrum published in a recent work from our group.<sup>6</sup> The  $^1\text{H}$  NMR spectrum of PGA (see Figure S4) is characterized by a great number of overlapped signals spanning from 2.92 to 1.97 ppm, which can be attributed to  $\beta$ - $\text{CH}_2$  and  $\gamma$ - $\text{CH}_2$  signals of the PGA backbone derived from different branching pathways, given its  $\text{AB}_2$  monomer nature. A specific attribution is not straightforward because two carboxylic groups and one amino group can form not only linear and branched peptide-like structures but also mixtures of both. The signals at 4.40 and 4.17 ppm can be attributed to the  $\alpha$ -CH proton being involved in branched and linear moieties. Figure S5 shows the  $^1\text{H}$  NMR spectrum of the polymer obtained by copolymerization of an equimolar amount of Glu and Lys (Glu–Lys 1:1) in the region 1.00–5.00 ppm, although a clear assignment is hampered by the simultaneous presence of different species whose signals are overlapped.

Given the problems encountered in analyzing the 1D NMR spectrum, the structure of the GluLys heteropolymer was studied by a  $^1\text{H}$ – $^{13}\text{C}$  NMR HSQC bidimensional heteronuclear correlation (Figure 4). Despite the low resolution of the spectrum, especially the carbon, mostly due to the great number of cross reactions that can occur between  $\text{AB}_2$  (Glu) and  $\text{A}_2\text{B}$  (Lys) monomers, it is possible to make a tentative attribution of the signals with the support of similar structures reported in the literature.<sup>26</sup> Starting from the low field, we can attribute the couple of paired signals at 4.11–59.76 and 4.02–59.76 ppm to the branched and linear  $\alpha$ -CH of Lys and those at 3.94–57.02 and 3.90–57.02 ppm to the  $\alpha$ -CH of Glu. The couple of paired signals at 2.96–41.76 and 2.74–41.75 ppm

can be clearly assigned, respectively, to the branched and linear  $\epsilon$ -Lys. Since the methylene protons of Glu rarely shift to values lower than 2 ppm, the signals at 2.16–31.98 can be attributed to  $\gamma$ -Glu, while the  $\beta$ -Glu methylene group exhibited two different signals: 2.27–28.06 and 1.77–28.06. The remaining signals can be attributed to the Lys side chain:  $\beta$ -Lys (1.28–30.80 ppm),  $\gamma$ -Lys (1.06–22.98 ppm), and  $\delta$ -Lys (1.57–35.50 ppm). The NMR data clearly indicate that the Glu–Lys copolymer has a branched nature.

XRD analyses were performed on the GluLys 1:1 sample obtained with three different thermal treatments (180, 220, and 240 °C) (Figure S6a) and on GluLys 1:1 and 2:1 polymers obtained at 240 °C (Figure S6b) to assess the crystalline nature of the polymers. As expected, all of the samples were characterized by a single broad signal centered at  $2\theta = 20.2^\circ$ , distinctive of amorphous carbon-based polymeric materials.<sup>27</sup> The XRD amorphous patterns, together with the absence of aromatic signals in the NMR analysis, lead to the conclusion that the fluorescence emission of our samples (see below) cannot be ascribed to the presence of some graphitic core, but it needs to be explained through different emission pathways.

The morphology of the polymers was studied through transmission electron microscopy (TEM). Figure 5 shows the bright-field representative images of the GluLys 1:1 (a) and GluLys 2:1 (b) samples with the related size distribution in the insets.

The sample obtained with an equimolar amount of Glu and Lys is characterized by spheroidal nanoparticles with a rugged surface, whose average size is 110 nm, while the sample achieved with a Glu:Lys molar ratio of 2:1 features a similar shape but an average size of 30 nm. In both cases, it is possible to indicate the tendency of the particles to aggregate in clusters despite the ultrasonication treatment they underwent before deposition and analysis. Due to technical issues related to the chemical nature of the sample, it was not possible to acquire an accurate bright-field image of PGA (Figure S7). In fact, after casting the PGA dispersion in water onto the carbon-coated copper grid, the material formed a homogeneous layer that cracked while drying.

The optical properties of Lys homopolymers obtained through a solventless thermal procedure, and in particular the photoluminescence (PL), have been largely investigated by our group, with and without the support of boric acid as an amidation catalyst.<sup>2,6</sup> Moreover, these properties have also been explored on homopolymers achieved through a hydrothermal procedure by controlling the protonation state of Lys.<sup>11</sup> The present work aimed instead at investigating the PL properties of heteropolymers obtained by coupling different molar ratios of Lys with another biologically very important AB<sub>2</sub> amino acid, Glu, which, as mentioned above, is somehow the counterpart of Lys. After the synthesis, we compared the optical properties of the Glu–Lys heteropolymer with those of the two separated homopolymers: hyperbranched polylysine (PolyLys)<sup>2</sup> and polyglutamic acid (PGA). Figure 6 shows the UV–vis absorption spectra in the 200–500 nm region of the two monomers, Glu and Lys, the PGA polymer, and the heteropolymer obtained by polymerizing Glu–Lys in a 1:1 ratio. The absorption profile indicates that Glu does not have any appreciable absorption compared to the Lys monomer, which instead exhibits a weak broad absorption band peaking at around 280 nm. In PGA, the absorption band is red-shifted to 300 nm, while the Glu–Lys 1:1 polymer displays a well-defined band centered at 330 nm. Both absorption bands can

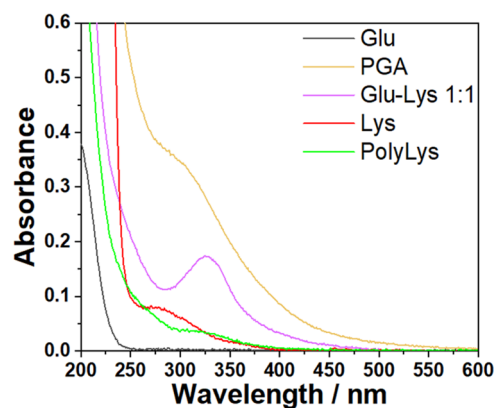


**Figure 6.** Optical absorption (UV–vis) spectra of L-glutamic acid (Glu), polyglutamic acid (PGA) homopolymer, glutamic acid:lysine (GluLys 1:1) copolymer, L-lysine (Lys), and polylysine (PolyLys) homopolymer in aqueous solutions.

be correlated to  $n-\pi^*$  transitions due to the abundance of C=O groups involved in peptide bonds.

The photoluminescence (PL) of the different polymers was mapped by 3D emission–excitation–intensity graphs (Figure 7), which revealed a surprisingly different behavior of the Glu–Lys heteropolymer with respect to both the homopolymers generated by the single monomers, PGA and Poly-Lys. The 3D PL map of a 0.034 M aqueous solution of the Glu monomer (Figure 7c) has been added as a reference. It shows that, in solution, Glu is not fluorescent, although we have experimentally verified that it exhibits a very weak fluorescence in the solid state. The 3D PL map of a 0.1 M aqueous solution of the Lys monomer (Figure 7f) shows instead, as expected, a weak emission.<sup>28</sup>

Homopolymers PGA and Poly-Lys present a single distinct emission in the blue region. PGA (Figure 7a) emits at around 435 nm when excited at 365 nm; Poly-Lys (Figure 7e) emits at 460 nm when excited at 350 nm. Surprisingly, thermal copolymerization of Glu and Lys produces two centers of excitation-dependent fluorescence (Figure 7d). One lies in the same range of excitation–emission wavelengths of the homopolymers (emitting at 450 nm when excited at 380 nm), while the new one has an emission maximum at about 390 nm when excited at 330 nm. The latter excitation can be easily correlated with the absorption associated with the  $n-\pi^*$  transition that appeared in the UV–vis spectrum of Glu–Lys 1:1 (see Figure 6). Scheme 3 shows a drawing of possible structures of 1:1 PGA, PolyLys, and Glu–Lys 1:1.

To rule out the possibility that the emission at 390 nm originated from the interaction of a mixture of two discrete homopolymers, PGA and PolyLys, we acquired a 3D PL map of an aqueous solution obtained by mixing an equal amount (0.03 mg mL<sup>-1</sup>) of the two homopolymers. The resulting 3D map (Figure 7b) shows only a single fluorescent emission associated with the homopolymers and thus clearly highlights that the aforementioned emission cannot be originated by simple interactions occurring between the two discrete homopolymers. Moreover, to make sure that this emission is a peculiar property of the GluLys copolymers, an additional experiment was performed by mixing the PGA polymer (0.03 mg mL<sup>-1</sup>) with two different concentrations of the Lys monomer: 0.1 M (Figure S8c) and 1 M (Figure S8d). In both cases, the 3D PL maps indicated the presence of a single fluorescent emission centered at 450 nm with a stronger

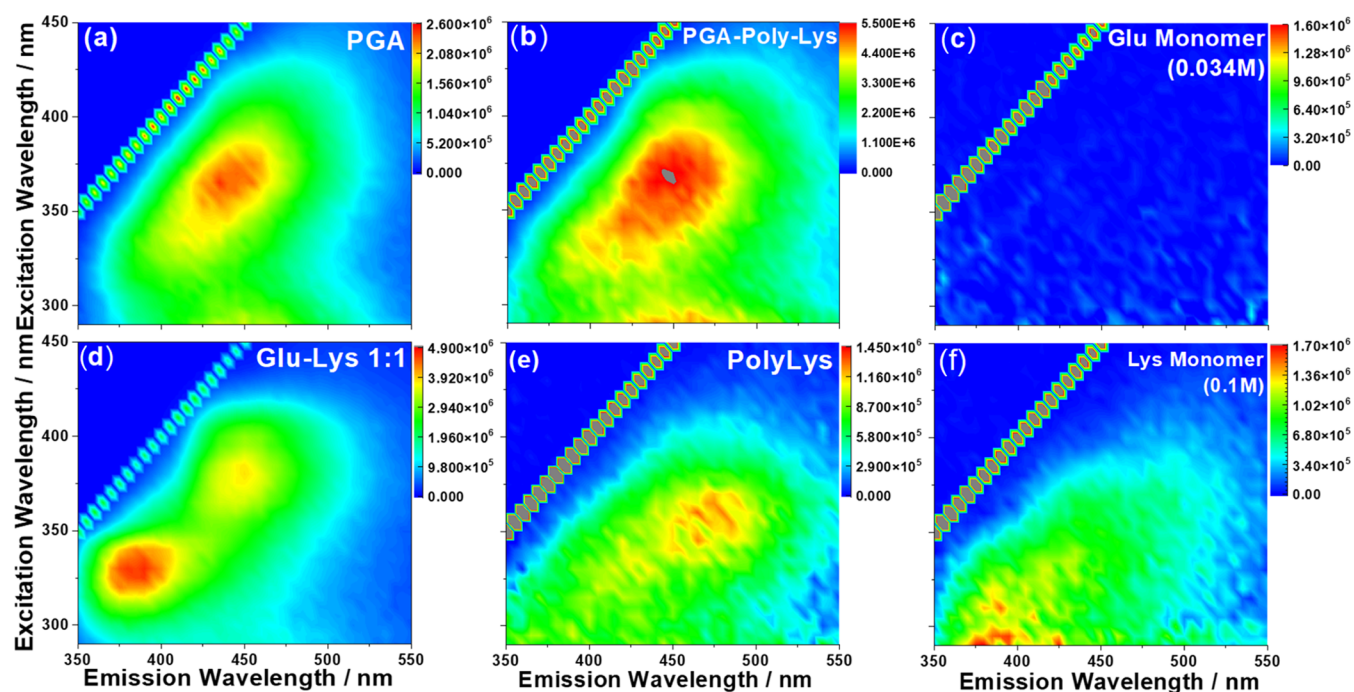
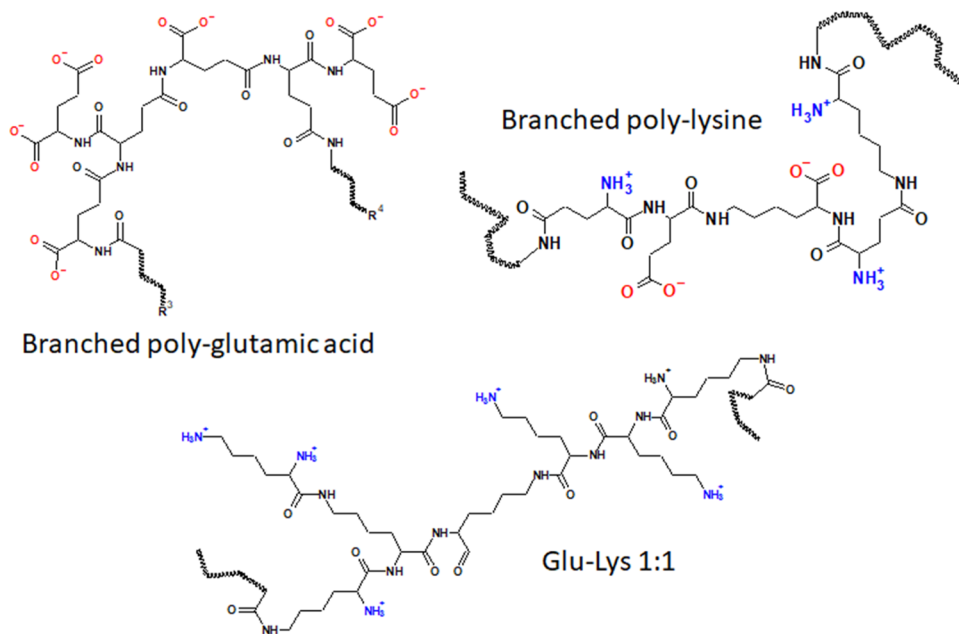


**Figure 7.** Excitation ( $y$ )–emission ( $x$ )–intensity ( $z$ ) 3D PL maps of PGA (a), 1:1 mix of PGA and Poly-Lys polymers ( $0.03 \text{ mg mL}^{-1}$ ) (b), Glu monomer ( $0.034 \text{ M}$ ) (c), Glu–Lys 1:1 polymer (d), Poly-Lys polymer (e), and Lys monomer  $0.1 \text{ M}$  (f). The polymer concentration was equal to  $0.03 \text{ mg mL}^{-1}$  in Milli-Q water. The intensities are given in a false color scale.

### Scheme 3. Possible Structures of Branched Polyglutamic Acid, Branched Poly-Lysine, and Glu–Lys 1:1 Polymers



emission at higher concentrations of the Lys monomer. After establishing a necessary relationship of the dual emission with the GluLys copolymer, attention has been drawn to develop a possible correlation with the heating process. To understand how thermal treatment could affect the origin of this double emission, Glu and Lys were polymerized in a 1:1 ratio for 5 h at increasing temperatures: 140, 180, 220, and 240 °C. The optical properties of the resulting polymers were characterized by UV–vis absorption spectra and 3D photoluminescence maps (Figure 8).

The 3D PL maps of Figure 8a–d show how the excitation-dependent fluorescence of 1:1 Glu–Lys changes as a function of the polymerization temperature. The treatment at 140 °C produces only the broad single emission typical of the homopolymers, although still weak. After increasing the temperature to 180 °C, the dual fluorescence is still in its embryonic stage but with a broader extension. However, it starts to be envisaged at 220 °C, and it can be clearly detected only at 240 °C. A similar trend can be found in the UV–vis absorption spectra (Figure 8e). The absorption band centered at 330 nm (vide supra) slowly increases in intensity as a



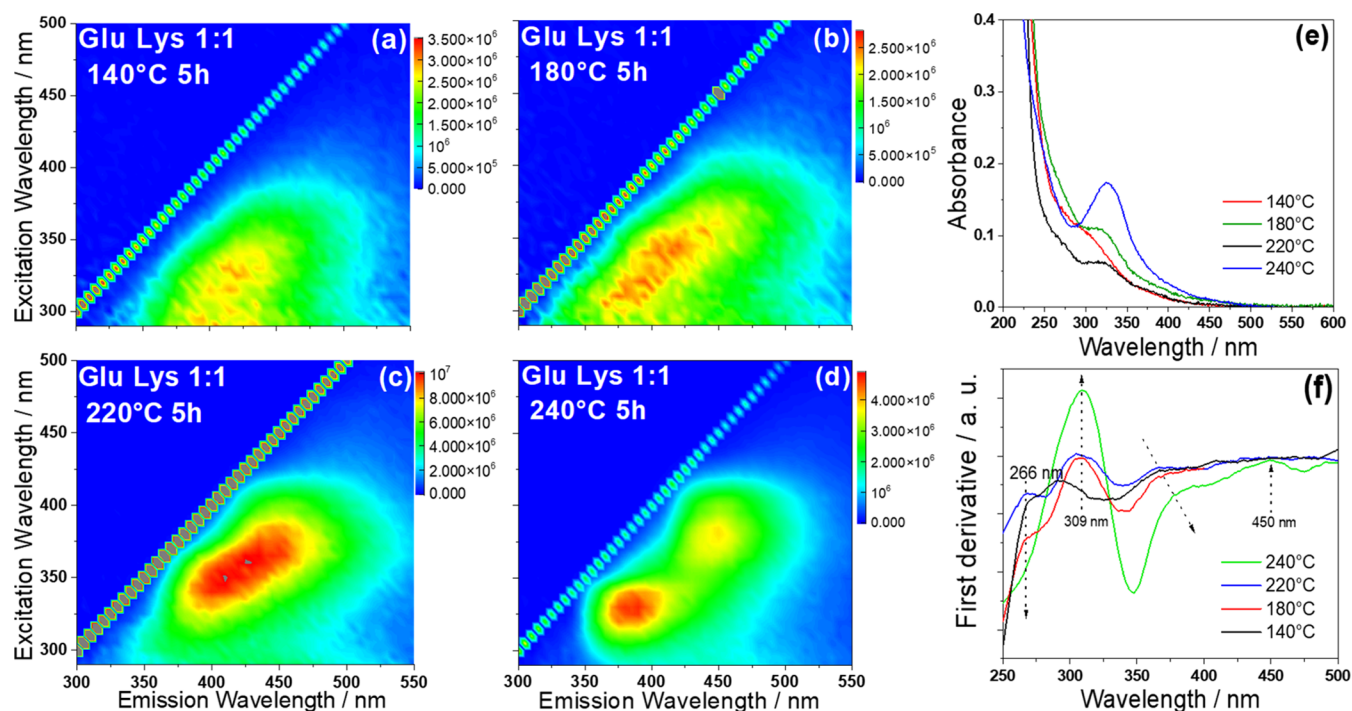


**Figure 8.** Excitation ( $y$ )–emission ( $x$ )–intensity ( $z$ ) 3D fluorescence maps of Glu–Lys 1:1 at 140 °C (a), 180 °C (b), 220 °C (c), and 240 °C (d). The samples were dissolved in water with a concentration of  $0.03 \text{ mg mL}^{-1}$ . The intensities are given in a false color scale. Optical absorption (UV–vis) spectra of Glu–Lys 1:1 polymers at 140, 180, 220, and 240 °C (e). First derivatives of the UV–vis spectra (f). The arrows indicate the direction of change with an increase in the temperature.

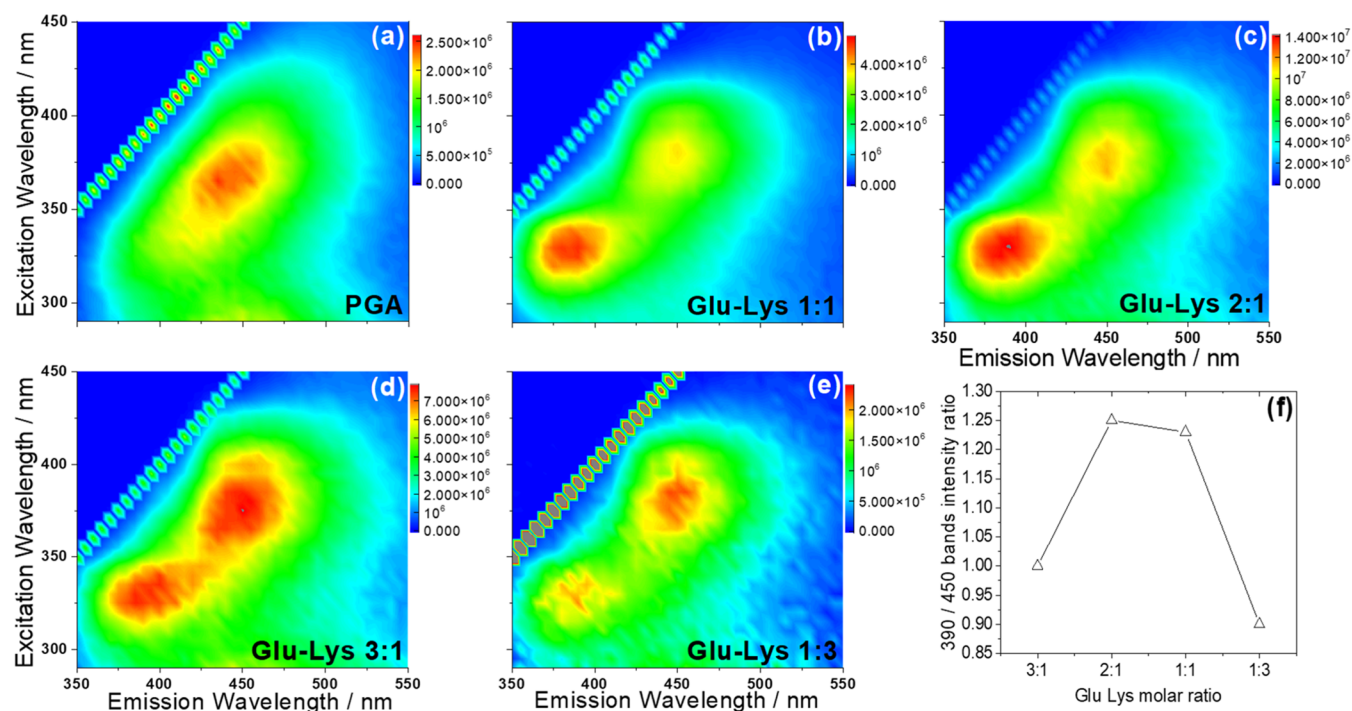


**Figure 9.** Excitation ( $y$ )–emission ( $x$ )–intensity ( $z$ ) 3D fluorescence maps of PGA (a), Glu–Lys 1:1 (b), Glu–Lys 2:1 (c), Glu–Lys 3:1 (d), and Glu–Lys 1:3 (e) and change of the peak intensity ratio of the two emission centers ( $\lambda_{\text{ex}} = 330 \text{ nm}$  and  $\lambda_{\text{ex}} = 450 \text{ nm}$ ) (f).

function of the temperature, becoming a distinct band at 240 °C. This temperature is linked with the polymerization of Lys, which occurs at a later stage with respect to Glu. In the present case, the formation of a highly interconnected and branched polymer appears as a condition for the rise of the emission through energy charge transfer between close side chains. This

is why the intensity of the emission is strictly correlated to the polymerization that, on turn, is controlled by the temperature of the treatment. Figure 8f shows the first derivative curves of the absorption spectra. They reveal the presence of four bands at around 266, 309, 350–370, and 450 nm. The first one is assigned to  $\pi$ – $\pi^*$  transitions and does not emit; the 309 and

350–370 nm bands are due to  $n-\pi^*$  transitions and correlated to the first and second emission centers, respectively. The last one is observed only in the sample treated at 240 °C and is not emissive. Interestingly, the Stokes shift in the lower energy band is at around 4500 and 4100  $\text{cm}^{-1}$  for the higher-energy emission in the near-UV region. The similar Stokes shift suggests that the emission mechanism could have a similar origin.

Figure 8 shows that thermal copolymerization of the two amino acids induces the formation of two-color centers. The origin of the emission is thus connected to the polymer structure resulting from the amide reactions that lead to an interconnected structure of Glu and Lys. The thermal homopolymerization process in Glu and Lys creates similar blue-emitting color centers, as shown in Figure 7a,e. Therefore, the origin of such fluorescence should be similar and favored by the branching process during polymerization. In previous work,<sup>2</sup> we attributed the emission of hyperbranched polylysine to the inhibition, from the polymeric network, of nonradiative recombinations induced by molecular motions. Intramolecular hydrogen bonding promotes intermolecular interaction and causes specific emission upon thermal polymerization and formation of branched structures. This mechanism, which explains the blue emission in Poly-Lys, can also be adopted to describe the blue emission in PGA. However, the origin of the intense emission at smaller wavelengths detected in the copolymer has a different root.

The effect of the copolymerization of Glu and Lys on the fluorescence emission was investigated by preparing various heteropolymers characterized by different molar ratios of the two precursors spanning from 3:1 to 1:3. Figure 9 shows the excitation ( $y$ )–emission ( $x$ )–intensity ( $z$ ) 3D fluorescence maps of PGA (Figure 9a) and GluLys polymers in different molar ratios: 3:1 (b), 2:1 (c), 1:1 (d), and 1:3 (e). The false color scale of each 3D map was chosen to emphasize the relative intensities of the two emission centers.

Figure 9f shows the intensity ratios of the two emission peaks (upon excitation at 330 and 380 nm) for each molar ratio. PGA is reported as a reference and, as discussed before, shows only one component emission at higher wavelengths as well as thermally polymerized Lys (Figure 7e). This component is therefore connected to the formation of the branched Glu and Lys homopolymers. Figure 9f clarifies how the relative intensity of the two emission bands changes in accordance with the relative molar ratio (see also Figure S9). Interestingly, in the intermediate compositions, Glu–Lys 2:1 and Glu–Lys 1:1, the components have a similar emission intensity, while at the two extremes, Glu–Lys 3:1 and Glu–Lys 1:3, the intensity of the components at longer wavelengths increases. The excess of either Lys or Glu induces a larger emission of the component, which is observed in the homopolymers. This finding indicates that the second emission center is strictly correlated with a tight interaction between Glu and Lys backbones.

The quantum yields (QYs) of the PGA and GluLys polymers were measured for both fluorescent emissions, and the results are reported in Table 1.

Although the QYs reported in Table 1 do not indicate a clear correlation between the polymer QYs and molar ratios of the two precursors, we can try to make some kind of correlation by looking at the values for the emission at 450 nm. In fact, the QY seems to decrease by reducing the amount of Glu from 5.01% (PGA) to 3.00% (GluLys 2:1) but greatly

**Table 1. Quantum Yields (QYs) for the PGA Polymer Single Emission and Glu–Lys Heteropolymers in the Molar Ratios of 3:1, 2:1, and 1:1**

sample	$\lambda_{\text{em}} = 380 \text{ nm}$	$\lambda_{\text{em}} = 450 \text{ nm}$
PGA		5.01
Glu–Lys 3:1	4.93	4.88
Glu–Lys 2:1	3.11	3.00
Glu–Lys 1:1	3.03	9.12

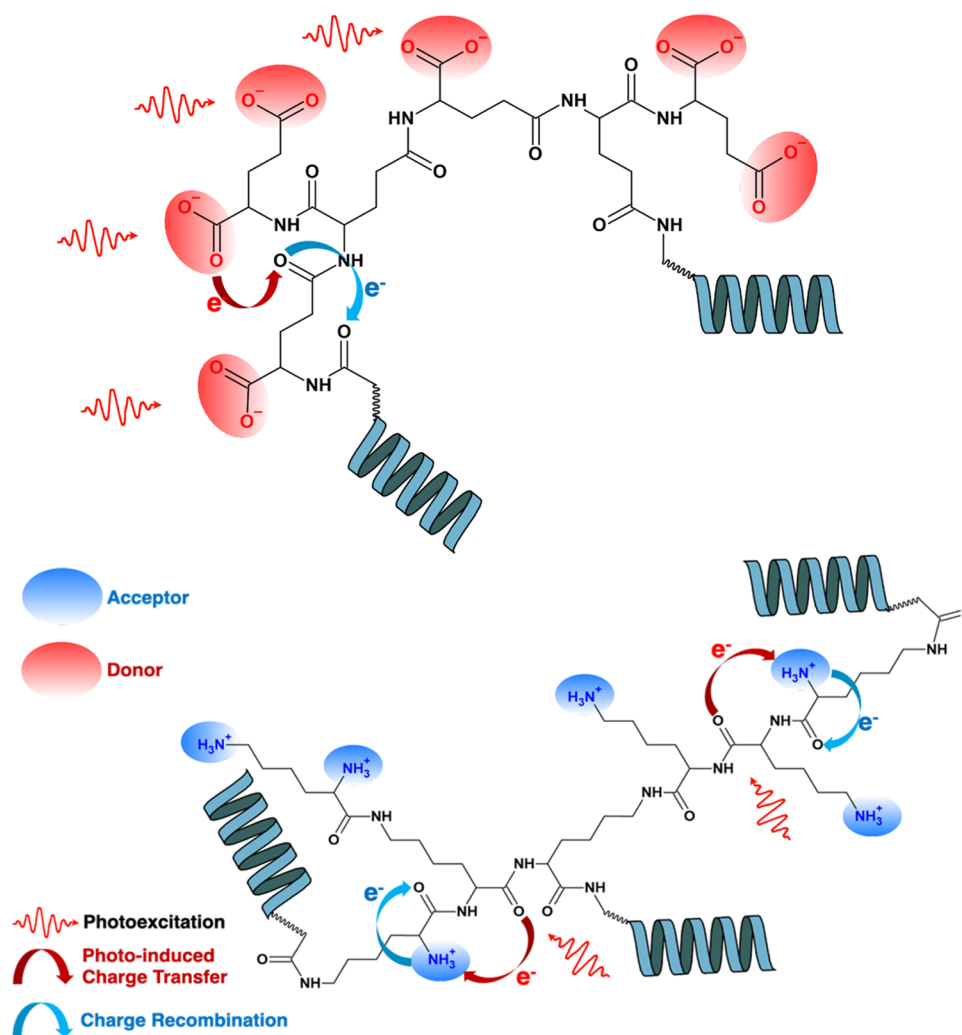
increases for GluLys 1:1, reaching 9.12%. Interestingly, this value is higher than that obtained in our previous work for the hyperbranched polylysine (7.4%),<sup>2</sup> suggesting that thermal copolymerization of the two precursors gives rise to a more efficient system compared to their homopolymers. In the case of the fluorescence emission at 380 nm, it is not possible to make a direct comparison of QY with samples other than those we have prepared. The study of the fluorescent QY of hyperbranched polymers obtained via thermal polymerization, to the best of our knowledge, is not very common. Nevertheless, also for this emission, it is possible to evidence that an increase in the Lys monomer produces a slight decrease of the QY efficiency (from 4.93 to 3.03%). Curiously, the GluLys 1:1 sample displays the higher gap between the two QYs.

## DISCUSSION

The formation of two emission centers in the Glu–Lys copolymers is quite surprising even if blue-green fluorescent emissions of nonaromatic species has been observed in different biopolymers, which are mostly characterized by amyloid-like structures.<sup>29</sup> These structures show an optical absorption in the near-UV range and a correlated fluorescence due to  $n \rightarrow \pi^*$  transitions involving a great number of carbonyl moieties of the amide groups. Usually, photoexcitation stimulates a charge transfer from a donor to an acceptor group where a charge recombination results in a fluorescent emission. Occasionally, charge transfer could involve an intermediate species that mediates the transfer before recombination occurs. This mechanism can be of two types, depending upon the abundance of specific functional groups, and they can be explained by two different molecular routes.<sup>1,5</sup> The first involves the amide groups of the peptide backbone that can act as both a donor and an acceptor depending on the packing structure. The supramolecular assembly of the amino acids in fact greatly affects the optical properties of the resulting polymers. Moreover, this mechanism can be strengthened by the presence of positively charged species such as ammonium moieties. This molecular path is characterized by optical absorption in the 340–400 nm range, and it leads to emission in the 440–530 nm interval. To the best of our knowledge, the first example of this emission in a synthetic proteinoid was reported by our group while studying the fluorescent emission of hyperbranched polylysine obtained through thermal polymerization with<sup>6</sup> and without<sup>2</sup> the support of boric acid as the catalyst. In this case, the excitation-dependent emission of the L-lysine monomer that at high concentrations becomes weakly fluorescent ( $\lambda_{\text{em}} = 415 \text{ nm}$ ),<sup>30</sup> exhibiting a stronger blue emission at 450 nm once converted into a hyperbranched polymer.

Scheme 4 (Bottom) shows the molecular pathways through which donor amide groups of the hyperbranched polylysine underwent photoexcitation, transferring a charge to nearby

Scheme 4. Molecular Pathways of Photoexcitation, Photoinduced Charge Transfer, and Charge Recombination in Polyglutamic Acid (Top) and Hyperbranched Polylysine (Bottom)



ammonium groups. These groups, in turn, induced a charge recombination onto a neighboring amide acceptor, thus giving rise to the single blue emission. This result agrees with the electronic structure calculations performed by Prasad et al., who demonstrated that the charge transfer involves the Lys backbone and its ammonium residues.<sup>31</sup> These positively charged moieties make available unoccupied molecular orbitals, thus populating the amino groups with charge acceptor states.

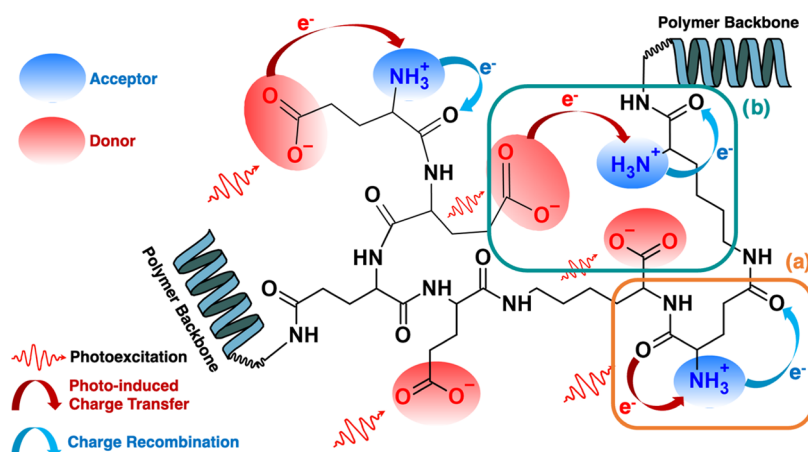
A similar molecular route can also be hypothesized in the case of the PGA polymer synthesized in the present work, with a significant difference in the presence of an excess of carboxylate groups that can act as a charge donor upon irradiation. The PGA homopolymer structure shows optical absorption below 320 nm, which can be related to a  $n \rightarrow \pi^*$  transition (Figure 8e). The maximum of fluorescent emission of PGA can be obtained by exciting the polymer at 365 nm, which corresponds to a single maximum at 435 nm. This result can be thus explained by a mechanism similar to that accountable for the hyperbranched polylysine emission and that involves mainly the peptide backbone assembly. However, a significant difference lies in the groups capable of triggering the fluorescent emission since the negatively charged

carboxylate moieties, characterizing the PGA polymer, are electron-rich groups with occupied molecular orbitals.

Xhang et al. supposed that the origin of fluorescence in PGA should be attributed to the chromophore character of the  $n \rightarrow \pi^*$  transition of the amide bond with some contribution from the intermolecular interactions, such as intramolecular hydrogen bonding.<sup>32</sup> This hypothesis is, however, in contradiction with the optical response of the L-lysine monomer, which shows a concentration-dependent fluorescence in solution with an emission peaking at 440 nm without the need for amide bonds.<sup>28</sup> Intermolecular interactions and not the amide bonds should therefore be the main source of fluorescence even in branched polymers from Lys and Glu amino acids. On the other hand, the in situ analysis by FTIR and the 3D fluorescence maps recorded for samples treated at different temperatures show that the 450 nm fluorescence increases before the amidation reaction starts (Figure 3). This fluorescence is due to charge transfer mechanisms similar to those observed for Lys at high concentrations. The amount of amidic bonds governs the polymerization stage when the close packing of the chains favors the photoactivated charge transfer.

Scheme 4 (Top) illustrates how the photoexcited carboxylate groups can transfer a charge to an amide acceptor, which in turn transfers its charge to another acceptor amide through a

**Scheme 5. Molecular Pathways of Photoexcitation, Photoinduced Charge Transfer, and Charge Recombination in Glu–Lys 1:1 Polymer: Molecular Pathway of the Charge Transfer Accountable for the Blue Emission (450 nm) (a) and Charge Transfer Mechanism between Oppositely Charged Moieties That Explains the Emission in the Near-UV (390 nm) Region (b)**



charge recombination path.<sup>31</sup> Some differences between the optical properties of PGA and hyperbranched polylysine, besides the opposite charges, must be found in the shorter side chain length of Glu and the presence of lone pairs onto its carboxylate residues. According to data from the literature, charge transfer occurs often in Lys- and Glu-rich proteins. Our research team also noticed this property in branched polymers made by thermally copolymerizing the two amino acids. Moreover, the present study of heteropolymers obtained by combining two amino acids in different molar ratios afforded valuable insights into the origin of excitation-dependent emission provided by the combination of these two residues. This finding confirms some of the conclusions obtained by other groups on the properties of nonaromatic polypeptide rich in Glu and Lys residues. In particular, we have discovered that thermal copolymerization of Glu and Lys monomers forms a heteropolymer featuring two fluorescent emissions. The first emission, centered at around 450 nm when excited at 380 nm, substantially overlaps with the emission of Lys and Glu homopolymers (see Figure 6). The 450 nm emission can be correlated with the photoinduced charge transfer from the carboxylate moieties to the amide backbone (Glu–COO<sup>−</sup> → backbone) or from the amide backbone to the ammonium and back to the backbone (backbone → Lys–NH<sub>3</sub><sup>+</sup> → backbone). The second emission, centered at around 390 nm when excited at 330 nm, has a different origin, which can be explained through different molecular routes already supposed to work in monomeric proteins<sup>33</sup> rich in Glu and Lys residues.<sup>5</sup> Kumar et al. assumed that this peculiar emission should be correlated with the formation of strong salt bridges between oppositely charged residues, such as Lys and Glu, which are capable of photoinduced charge transfer.<sup>29</sup> This led to the conclusion that the emission was starkly correlated with paired ionized residues in close spatial proximity. Pinotsi et al. explained the origin of this fluorescence emission through the formation of a strong hydrogen bond (SHB) between the N-termini or C-termini of peptides.<sup>34</sup> The proton transfer, in fact, lowers the excitation energy levels, shifting the absorption toward the UV range. Both hypotheses could support the emission shown by our polymers since both can explain the strong interaction arising from the pairing of Lys and Glu residues.

Scheme 5 summarizes the possible charge transfer accountable for the origin of both emissions shown by Glu–

Lys heteropolymers. In fact, the emission centered at around 450 nm and correlated to the amide backbone can be explained through the mechanism already discussed above for the Glu and Lys homopolymers (vide supra) and schematized in pitch (a). A photoexcited amide group acts as a donor, transferring a charge to an ammonium residue that, in turn, transfers its charge to an acceptor amide. The final charge recombination produced fluorescent blue emission (450 nm). The emission in the near-UV region (centered at around 390 nm) can be explained with the hypothesis that the strong interaction between the oppositely charged residues produces a neutral moiety, given by the formation of a salt bridge that restricts the spectral range in which the charge transfer occurs. Pitch (b) of Scheme 5 clarifies the mechanism associated with salt bridge formation. The photoinduced charge transfer from a carboxylate to an ammonium group is made easier by the close acceptor–donor spatial proximity. The first charge transfer is followed by a charge recombination from the ammonium to an amide backbone acceptor, which is associated with the near-UV fluorescence emission (see Figure 9).

It is noteworthy that, to the best of our knowledge, the Glu–Lys polymers of the present work are the first examples of proteinoids exhibiting nonaromatic fluorescence obtained through thermal polymerization. The polymers feature dual emission fluorescence in the near-UV (390 nm) and blue (450 nm) ranges, whose intensity can be controlled by the relative molar ratio of the precursor monomers, Glu and Lys.

## CONCLUSIONS

Polypeptide-like branched polymeric structures have been synthesized via the thermal treatment of L-lysine and L-glutamic acid. Thermal polymerization produces branched polymers whose close packing between the chains favors intramolecular charge transfer. The polymers exhibit two-color centers with emissions peaking at around 380 and 450 nm. The relative homopolymers, polyglutamic acid and polylysine, exhibit, upon thermal polymerization, only one emission at 450 nm. The second emission is observed only when the two amino acids are copolymerized. The polymerization kinetics and, thus, the incorporation and abundance of the precursors into the final polymers affect their spatial conformation, which is starkly correlated to the relative molar ratios of the two precursors. The structural characterization has shown that the

increase of fluorescence is strictly correlated with the mutual spatial proximity of oppositely charged moieties, which favors charge transfer between the side chains of the precursor amino acids.

## ■ ASSOCIATED CONTENT

### SI Supporting Information

The Supporting Information is available free of charge at <https://pubs.acs.org/doi/10.1021/acs.macromol.3c01825>.

Content of Supporting Information: Table S1, Yields of thermal polymerization calculated on the raw material and after filtration and dialysis; Figure S1, FTIR absorption spectra of the pure amino acids in the crystalline form; Table S2, FTIR vibrational modes of L-Glu in the crystalline state; Table S3, FTIR vibrational modes of L-Lys in the crystalline state; Figure S2, FTIR absorption spectra of the PGA polymer dialyzed and not dialyzed, PGA polymer dialyzed, Glu–Lys 1:1 polymer dialyzed and not dialyzed, and d) Glu–Lys 1:1 polymer dialyzed; Figure S3,  $^1\text{H}$  NMR spectrum of the L-Glu monomer in  $\text{D}_2\text{O}$ ; Figure S4,  $^1\text{H}$  NMR spectrum of PGA in  $\text{D}_2\text{O}$ ; Figure S5,  $^1\text{H}$  NMR spectrum of the Glu–Lys 1:1 polymer in  $\text{D}_2\text{O}$ ; Figure S6, XRD patterns of GluLys polymers as a function of the temperature and Glu:Lys molar ratio; Figure S7, Bright-field images of PGA acid; Figure S8, Excitation ( $y$ )–emission ( $x$ )–intensity ( $z$ ) 3D map of PGA, PGA–PolyLys 1:1, PGA–Lys monomer 0.1 M, and PGA–Lys monomer 1 M; Figure S9, emission bands of Glu–Lys 3:1, Glu–Lys 2:1, Glu–Lys 2:1, and Glu–Lys 1:3 (PDF)

## ■ AUTHOR INFORMATION

### Corresponding Authors

**Davide Carboni** – *Laboratorio di Scienza dei Materiali e Nanotecnologie (LMNT), CR-INSTM, Dipartimento di Scienze Biomediche, Università di Sassari, 07100 Sassari, Italy*; [orcid.org/0000-0003-2499-4567](https://orcid.org/0000-0003-2499-4567); Email: [dcarboni@uniss.it](mailto:dcarboni@uniss.it)

**Plinio Innocenzi** – *Laboratorio di Scienza dei Materiali e Nanotecnologie (LMNT), CR-INSTM, Dipartimento di Scienze Biomediche, Università di Sassari, 07100 Sassari, Italy*; [orcid.org/0000-0003-2300-4680](https://orcid.org/0000-0003-2300-4680); Email: [plinio@uniss.it](mailto:plinio@uniss.it)

### Authors

**Marta Cadeddu** – *Laboratorio di Scienza dei Materiali e Nanotecnologie (LMNT), CR-INSTM, Dipartimento di Scienze Biomediche, Università di Sassari, 07100 Sassari, Italy*; [orcid.org/0009-0000-5287-834X](https://orcid.org/0009-0000-5287-834X)

**Luigi Stagi** – *Laboratorio di Scienza dei Materiali e Nanotecnologie (LMNT), CR-INSTM, Dipartimento di Scienze Biomediche, Università di Sassari, 07100 Sassari, Italy*; [orcid.org/0000-0002-7238-8425](https://orcid.org/0000-0002-7238-8425)

**Luca Malfatti** – *Laboratorio di Scienza dei Materiali e Nanotecnologie (LMNT), CR-INSTM, Dipartimento di Scienze Biomediche, Università di Sassari, 07100 Sassari, Italy*; [orcid.org/0000-0001-6901-8506](https://orcid.org/0000-0001-6901-8506)

**Maria F. Casula** – *Dipartimento di Ingegneria Meccanica, Chimica e dei Materiali, Università di Cagliari, 09123 Cagliari, Italy*; [orcid.org/0000-0002-2973-0002](https://orcid.org/0000-0002-2973-0002)

**Francesca Caboi** – *Laboratorio NMR e Tecnologie Bioanalitiche, Sardegna Ricerche, Parco Scientifico e tecnologico della Sardegna, 09010 Cagliari, Italy*

Complete contact information is available at:

<https://pubs.acs.org/10.1021/acs.macromol.3c01825>

### Author Contributions

M.C. synthesized and analyzed the materials, performed the characterizations, and reviewed the draft; D.C. conceived the study, designed and supervised the experiments, analyzed the data, and wrote and reviewed the draft; L.S. conceived the study, designed and supervised the experiments, acquired QYs and XRD patterns, and analyzed the data; M.F.C. acquired the TEM images; L.M. analyzed the TEM images; F.C. acquired the NMR spectra; P.I. supervised the study, wrote the draft, and reviewed the paper with the contribution from all authors. All authors have approved the final version of the manuscript.

### Notes

The authors declare no competing financial interest.

## ■ ACKNOWLEDGMENTS

This work has been developed within the framework of the project e.INS-Ecosystem of Innovation for Next Generation Sardinia (cod. ECS 00000038) funded by the Italian Ministry for Research and Education (MUR) under the National Recovery and Resilience Plan (NRRP)—MISSION 4 COMPONENT 2, “From research to business” INVESTMENT 1.5, “Creation and strengthening of Ecosystems of innovation” and construction of “Territorial R&D Leaders”. RAS with the support of Sardegna Ricerche is gratefully acknowledged for funding through POR FESR 2014–2020, project “PROOF of CONCEPT—CarDAVir”. The authors acknowledge the CeSAR (Centro Servizi Ricerca d’Ateneo) core facility of the University of Cagliari and Dr. Andrea Ardu for assistance with the generation of TEM images.

## ■ REFERENCES

- (1) Morzan, U. N.; Mirón, G. D.; Grisanti, L.; Lebrero, M. C. G.; Schierle, G. S. K.; Hassanal, A. Non-Aromatic Fluorescence in Biological Matter: The Exception or the Rule? *J. Phys. Chem. B* **2022**, *126*, 7203–7211, DOI: [10.1021/acs.jpcc.2c04280](https://doi.org/10.1021/acs.jpcc.2c04280).
- (2) Stagi, L.; Malfatti, L.; Caboi, F.; Innocenzi, P. Thermal Induced Polymerization of L-Lysine Forms Branched Particles with Blue Fluorescence. *Macromol. Chem. Phys.* **2021**, *222* (20), No. 2100242.
- (3) Stephens, A. D.; Qaisrani, M. N.; Ruggiero, M. T.; Schierle, G. S. K. Short hydrogen bonds enhance nonaromatic protein-related fluorescence. *Proc. Natl. Acad. Sci. U.S.A.* **2021**, *118* (21), No. e2020389118, DOI: [10.1073/pnas.2020389118](https://doi.org/10.1073/pnas.2020389118). May 17
- (4) Rodriguez, E. A.; Campbell, R. E.; Lin, J. Y.; Lin, M. Z.; Miyawaki, A.; Palmer, A. E.; Shu, X.; Zhang, J.; Tsien, R. Y. The growing and glowing toolbox of fluorescent and photoactive proteins. *Trends Biochem. Sci.* **2017**, *42* (2), 111–129, DOI: [10.1016/j.tibs.2016.09.010](https://doi.org/10.1016/j.tibs.2016.09.010).
- (5) Kumar, A.; Ahari, D.; Priyadarshi, A.; Ansari, Z. M.; Swaminathan, R. Weak Intrinsic Luminescence in Monomeric Proteins Arising from Charge Recombination. *J. Phys. Chem. B* **2020**, *124*, 2731–2746, DOI: [10.1021/acs.jpcc.9b10071](https://doi.org/10.1021/acs.jpcc.9b10071).
- (6) Stagi, L.; De Forni, D.; Malfatti, L.; Caboi, F.; Salis, A.; Poddesu, B.; Cugia, G.; Lori, F.; Galleri, G.; Innocenzi, P. Effective SARS-CoV-2 Antiviral Activity of Hyperbranched Polylysine Nanopolymers. *Nanoscale* **2021**, *13* (39), 16465–16476.
- (7) Tomalia, D. A.; Klajnert-Maculewicz, B.; Johnson, K. A. M.; Brinkman, H. F.; Janaszewska, A.; Hedstrand, D. M. Non-traditional intrinsic luminescence: inexplicable blue fluorescence observed for dendrimers, macromolecules and small molecular structures lacking

traditional/conventional luminophores. *Prog. Polym. Sci.* **2019**, *90*, 35–117.

(8) Chen, X.; Luo, W.; Ma, H.; Peng, Q.; Yuan, W. Z.; Zhang, Y. Prevalent intrinsic emission from nonaromatic amino acids and poly(amino acids). *Sci. China Chem.* **2018**, *61*, 351–359.

(9) Cossu, F. L.; Poddighe, M.; Stagi, L.; Anedda, R.; Innocenzi, P. The Birth of Fluorescence from Thermally Polymerized Glycine. *Macromol. Chem. Phys.* **2022**, *223*, No. 2200052, DOI: [10.1002/macp.202200052](https://doi.org/10.1002/macp.202200052).

(10) Hirayama, N.; Shirahata, K.; Ohashi, Y.; Sasada, Y. Structure of  $\alpha$ -form of L-glutamic acid.  $\alpha$ - $\beta$  transition. *Bull. Chem. Soc. Jpn.* **1980**, *53*, 30–35.

(11) Stagi, L.; Sini, M.; Carboni, D.; Anedda, R.; Siligardi, G.; Gianga, T. M.; Hussain, R.; Innocenzi, P. Modulating the Poly-L-Lysine Structure through the Control of the Protonation–Deprotonation State of L-Lysine. *Sci. Rep.* **2022**, *12* (1), No. 19719, DOI: [10.1038/s41598-022-24109-5](https://doi.org/10.1038/s41598-022-24109-5).

(12) Weiss, I. M.; Muth, C.; Drumm, R.; Kirchner, H. O. K. Thermal Decomposition of the Amino Acids Glycine, Cysteine, Aspartic Acid, Asparagine, Glutamic Acid, Glutamine, Arginine and Histidine. *BMC Biophys.* **2018**, *11* (11), No. 2, DOI: [10.1186/s13628-018-0042-4](https://doi.org/10.1186/s13628-018-0042-4).

(13) Nunes, R. S.; Cavalheiro, É. T. G. Thermal Behavior of Glutamic Acid and its Sodium, Lithium and Ammonium Salts. *J. Therm. Anal. Calorim.* **2007**, *87* (3), 627–630.

(14) Wu, H.; Reeves-McLaren, N.; Jones, S.; Ristic, R. I.; Fairclough, J. P. A.; West, A. R. Phase Transformations of Glutamic Acid and its Decomposition Products. *Cryst. Growth. Des.* **2010**, *10* (2), 988–994.

(15) Macklin, J. W.; White, D. H. Infrared spectroscopic studies of the effect of elevated temperature on the association of pyroglutamic acid with clay and other minerals. *Spectrochim. Acta* **1985**, *14*, 851–8591, DOI: [10.1016/0584-8539\(85\)80033-7](https://doi.org/10.1016/0584-8539(85)80033-7).

(16) Harada, K. Thermal Homopolymerization of Lysine and Copolymerization with Neutral and Acidic Amino Acids. *Bull. Chem. Soc. Jpn.* **1959**, *32*, 1007–1008.

(17) Mosqueira, F. G.; Ramos-Bernal, S.; Negrón-Mendoza, A. A simple model of the thermal prebiotic oligomerization of amino acids. *BioSystems* **2000**, *57*, 67–73, DOI: [10.1016/S0303-2647\(00\)00089-7](https://doi.org/10.1016/S0303-2647(00)00089-7).

(18) Martins, T. S.; Matos, J. R.; Vicentini, G.; Isolani, P. C. Synthesis, Characterization, Spectroscopy and Thermal of Rare Earth Picrate Complexes with L-Lysine. *J. Therm. Anal. Calorim.* **2005**, *82*, 77–82.

(19) Pokorný, V.; Štejfá, V.; Havlín, J.; Fulem, M.; Růžička, K. Heat Capacities of L-Cysteine, L-Serine, L-Threonine, L-Lysine, and L-Methionine. *Molecules* **2023**, *28* (1), No. 451, DOI: [10.3390/molecules28010451](https://doi.org/10.3390/molecules28010451).

(20) Dhamecourt, P.; Ramirez, F. J. Polarized Micro-Raman and Fourier Transform Infrared spectra of L-Glutamic acid. *J. Raman Spectrosc.* **1991**, *22*, 557–582, DOI: [10.1002/jrs.1250221007](https://doi.org/10.1002/jrs.1250221007).

(21) Pearson, J. F.; Slifkin, M. A. The infrared spectra of amino acids and dipeptides. *Spectrochim. Acta* **1972**, *28A*, 2408–2417, DOI: [10.1016/0584-8539\(72\)80220-4](https://doi.org/10.1016/0584-8539(72)80220-4).

(22) Navarrete, J. T. L.; Bencivenni, L.; Ramondo, F.; Hernández, V.; Ramirez, F. J. Structural and spectroscopical study of glutamic acid in the non-zwitterionic form. *J. Mol. Struct. Theochem* **1995**, *330*, 261–266, DOI: [10.1016/0166-1280\(94\)03848-F](https://doi.org/10.1016/0166-1280(94)03848-F).

(23) Roddick-Lanzilotta, A. D.; McQuillan, A. J. An in situ Infrared Spectroscopic Study of Glutamic Acid and of Aspartic Acid Adsorbed on TiO<sub>2</sub>: Implications for the Biocompatibility of Titanium. *J. Colloid Interface Sci.* **2000**, *227*, 48–54, DOI: [10.1006/jcis.2000.6864](https://doi.org/10.1006/jcis.2000.6864).

(24) Lin, S.-Y.; Yu, H.-L.; Li, M.-J. Formation of six-membered cyclic anhydrides by thermally induced intramolecular ester condensation in Eudragit E film. *Polymer* **1999**, *40*, 3589–3593.

(25) Nguyen, L. T.; Le Tran, H.; Mai, P. T.; Duong, V. B.; Nguyen, L. T. T.; Nguyen, H. T. Poly(L-Glutamic Acid) via Catalytic Hydrogenation for the Fabrication of Carbon Nanotube Nanocomposites. *Mater. Res.* **2021**, *24* (1), No. e20200321, DOI: [10.1590/1980-5373-mr-2020-0321](https://doi.org/10.1590/1980-5373-mr-2020-0321).

(26) Li, P.; Song, Y.; Dong, C.-M. Hyperbranched Polypeptides Synthesized from Phototriggered ROP of a Photocaged N<sub>ε</sub>-[1-(2-

Nitrophenyl)Ethoxycarbonyl]-L-Lysine-N-Carboxyanhydride: Microstructures and Effects of Irradiation Intensity and Nitrogen Flow Rate. *Polym. Chem.* **2018**, *9* (29), 3974–3986.

(27) Murthy, N. S.; Minor, H. General procedure for evaluating amorphous scattering and crystallinity from X-ray diffraction scans of semicrystalline polymers. *Polymer* **1990**, *31* (6), 996–1002.

(28) Stagi, L.; Farris, R.; de Villiers Engelbrecht, L.; Mocci, F.; Carbonaro, C. M.; Innocenzi, P. At the root of L-lysine emission in aqueous solutions. *Spectrochim. Acta, Part A* **2022**, *283*, No. 121717, DOI: [10.1016/j.saa.2022.121717](https://doi.org/10.1016/j.saa.2022.121717).

(29) Chan, F. T. S.; Schierle, G. S. K.; Kumita, J. R.; Bertoncini, C. W.; Dobson, C. M.; Kaminski, C. F. Protein Amyloids Develop an Intrinsic Fluorescence Signature During Aggregation. *Analyst* **2013**, *138*, 2156–2162, DOI: [10.1039/c3an36798c](https://doi.org/10.1039/c3an36798c).

(30) Homchaudhuri, L.; Swaminathan, R. Novel Absorption and Fluorescence Characteristics of L-Lysine. *Chem. Lett.* **2001**, *30*, 844–845.

(31) Prasad, S.; Mandal, I.; Singh, S.; Paul, A.; Mandal, B.; Venkatramani, R.; Swaminathan, R. Near UV-Visible Electronic Absorption Originating from Charged Amino Acids in a Monomeric Protein. *Chem. Sci.* **2017**, *8* (8), 5416–5433.

(32) Zhang, Z.; Yan, W.; Dang, D.; Zhang, H.; Sun, J. Z.; Tang, B. Z. The role of amide (n,  $\pi^*$ ) transitions in polypeptide clusteroluminescence. *Cell Rep. Phys. Sci.* **2022**, *3*, No. 100716, DOI: [10.1016/j.xcrp.2021.100716](https://doi.org/10.1016/j.xcrp.2021.100716).

(33) Lynch, M. Evolutionary diversification of the multimeric states of proteins. *Proc. Natl. Acad. Sci. U.S.A.* **2013**, *110* (30), E2821–E2828, DOI: [10.1073/pnas.1310980110](https://doi.org/10.1073/pnas.1310980110).

(34) Pinotsi, D.; Grisanti, L.; Mahou, P.; Gebauer, R.; Kaminski, C. F.; Hassanali, A.; Kaminski Schierle, G. S. Proton Transfer and Structure-Specific Fluorescence in Hydrogen Bond-Rich Protein Structures. *J. Am. Chem. Soc.* **2016**, *138* (9), 3046–3057.